



Highly selective acetone sensor based on ternary Au/Fe₂O₃–ZnO synthesized via co-precipitation and microwave irradiation

Yan LI, Li-li CHEN, Fang-xian ZHAO

College of Science, Civil Aviation University of China, Tianjin 300300, China

Received 3 July 2016; accepted 24 February 2017

Abstract: Ternary Au/Fe₂O₃–ZnO gas-sensing materials were synthesized by combining co-precipitation and microwave irradiation process. The as-prepared Au/Fe₂O₃–ZnO was characterized with X-ray diffractometer and scanning electron microscope, and its gas-sensing performance was measured using a gas-sensor analysis system. The results show that the as-prepared products consist of hexagonal wurtzite ZnO, face-centered cubic gold nanoparticles and orthorhombic Fe₂O₃ crystallines. The Au/Fe₂O₃–ZnO based sensor has a very high selectivity to ethanol and acetone, and also has high sensitivity (154) at a low working temperature (270 °C) and an extremely fast response (1 s) against acetone. It is found that the selectivity can be adjusted by Fe₂O₃ content added in the ternary materials. It possesses a worth looking forward prospect to practical applications in acetone detecting and administrating field.

Key words: zinc oxide; ferric oxide; gold; acetone sensor; ethanol sensor

1 Introduction

Gas sensitivity, as a typical application in detecting and monitoring systems, is receiving increasing attention in both industry and academia. Gas sensing technology has become more and more significant because of its widespread and common applications in many fields, such as industrial production, medical applications, and environmental studies [1,2]. Due to the different applicability and inherent limitations of different gas sensing technologies, researchers have been working on different methods to enhance gas sensitivity, selectivity and stability. Among all the gas-sensing materials, semiconducting metal oxides have great potential owing to the chemical interaction between gas molecules and the surface of semiconductor, which leads to changes in the electrical conductivity. Semiconducting metal oxides, such as ZnO, SnO₂, Fe₂O₃, CuO, WO₃ and V₂O₅, were used for gas sensing applications due to their electrical conductivity to the target gases [3–8]. As one of most important metal oxide semiconductor materials, ZnO has been considered as an excellent gas sensing material for the detection of both toxic and combustible gases, such as CO, H₂S, NH₃, acetone and ethanol [9–16]. In

principle, most gas sensors show high sensitivity to acetone [17,18], and considerable efforts have been made to improve the gas selectivity, such as decorating the materials with different elements [19–21]. YAN et al [22] prepared SnO₂–ZnO hetero-nanofibers by a facile electrospinning method and calcination, which has a good stability and excellent selectivity at the optimum temperature of 300 °C. The response and recovery time to 1×10⁻⁴ ethanol (volume fraction) were about 25 and 9 s, respectively. LI et al [23] reported that Au@ZnO yolk-shell nanospheres with a distinctive core@void@shell configuration have been successfully synthesized by deposition of ZnO on Au@carbon nanospheres. Its response to 1×10⁻⁴ acetone (volume fraction) was about 37, which was about 3 times higher than that of ZnO hollow (solid) nanostructures. HAN et al [24] prepared Fe-doped flowerlike ZnO powders with various doping contents by a hydrothermal method. The as-prepared Fe-doped ZnO showed excellent gas sensitivity, in which the gas response to 5×10⁻⁶ and 1×10⁻⁴ formaldehyde (volume fraction) can reach 22% and 287% under 532 nm light irradiation at room temperature, respectively. MIRZAEI et al [25] reported the synthesis of pristine α-Fe₂O₃ nanorods and Fe₂O₃–ZnO core-shell nanorods using a combination of

thermal oxidation and atomic layer deposition (ALD) techniques. The response of the core-shell nanorod sensor was 22.75 for 1×10^{-4} ethanol at 200 °C, whereas that of the pristine nanorod sensor was only 3.85 under the same conditions. Furthermore, under these conditions, the response time of the Fe₂O₃-ZnO core-shell nanorods was 15.96 s, which was shorter than that of the pristine nanorod sensor (22.73 s). Although some Au or Fe decorated ZnO binary species with high gas sensing to a few gases were reported, there is still less effective improvement on the gas selectivity. Preparing gas sensors with both high sensitivity and good selectivity becomes more important and imperative. It is widely expected that strategies based on improving gas sensing of samples, particularly from the selectivity, will have a great impact in gas detecting fields. Herein, we report a ternary Au/Fe₂O₃-ZnO NPs prepared via a facile method combining co-precipitation and microwave irradiation process.

2 Experimental

2.1 Synthesis of Au/Fe₂O₃-ZnO nanoparticles

Au/Fe₂O₃-ZnO was synthesized by a method combining co-precipitation and microwave irradiation. In a typical synthesized progress, 0.005 mol/L zinc chloride (ZnCl₂·5H₂O, A.R., 99%), 0.1 mol/L sodium hydroxide (NaOH, A.R., 96%), 0.01214 mol/L auric chloride acid (HAuCl₄, A.R., $w(\text{Au}) > 47\%$) solutions and 0.05 mol/L ferrous sulfate (FeSO₃·7H₂O, A.R., 99%) were first prepared, respectively. Then, the sodium hydroxide solution was dropwise added into the zinc chloride solution at a relatively low temperature (<10 °C). Then, the auric chloride acid solution and a certain ferrous sulfate solution were added into the mixture under a magnetic stirring at 2000 r/min for 2 h. The precipitates were retrieved by washing with distilled water and ethanol (C₂H₅OH, A.R., ≥99.7%) several times (≥3) and then irradiated under microwave field with a power of 700 W. The as-obtained samples were heat-treated in muffle furnace at 400 °C for 4 h. Finally, the solid products were collected for further characterization and measurement. Reagent usage for sample preparation is listed in Table 1. Samples ZFA-11, ZFA-12, ZFA-13,

ZFA-14, and ZFA-15 have Au to Zn molar ratio of 2%, and (Au + Fe) to Zn molar ratios of 0%, 5%, 15%, 20% and 30%, respectively.

2.2 Characterization and measurement

X-ray diffraction (XRD) analysis of as-prepared Au/Fe₂O₃-ZnO was characterized by employing a DX-2000 diffractometer (Dandong, Fang-Yuan Instrument Co., Ltd.) operating at 40 kV and 25 mA using Cu K_α ($\lambda=0.154184$ nm) radiation source employing a scanning rate of 0.1 (°)/s with 2θ ranging from 10° to 70°. The morphology was investigated using scanning electron microscopy (SEM, Hitachi, S-4800).

The fabrication procedures of gas sensor have been described in Ref. [26]. Dilute slurry composed of Au/Fe₂O₃-ZnO NPs and distilled water was coated onto an alumina tube with a diameter of 1 mm and a length of 4 mm, being positioned with a pair of Au electrodes and four Pt wires on both ends of the tube. A Ni-Cr alloy coil through the tube was employed as a heater to control the operating temperature. Finally, the gas sensors were dried in shade at room temperature for 24 h, and then anchored in an aging device at 80 mA for 24 h, followed by 180 mA for 2 h to get a quick heater-type ZnO gas sensor. The measurements were carried out on a chemical gas sensor-8 intelligent analysis system (Beijing Elite Tech Co., Ltd., China). The element gas sensitivity is defined as

$$R = R_a / R_g \quad (1)$$

where R_a is the electrical resistance measured in atmosphere (air), and R_g is the electrical resistance in air mixed with test gases.

3 Results and discussion

3.1 XRD and SEM analysis

Figure 1 shows XRD patterns of Au/Fe₂O₃-ZnO NPs. Diffraction peaks of all samples at 31.82°, 34.46°, 36.32°, 47.65°, 56.67°, 62.93° and 67.88° are ascribed to (100), (002), (101), (102), (110), (103) and (112) planes of ZnO, which can match with hexagonal wurtzite ZnO structure (JCPDS Card No. 36-1451). Diffraction peaks at 38.26° and 44.46° are attributed to the face-centered cubic crystalline Au (JCPDS Card No. 04-0784) and the orthorhombic crystalline Fe₂O₃ (JCPDS Card No. 47-1407), respectively. The diffraction intensities of ZnO decrease clearly with increasing Fe-decorating content. The average crystalline size (D) is estimated from the Debye-Scherrer equation:

$$D_{hkl} = 0.89\lambda / \beta \cdot \cos\theta \quad (2)$$

where λ represents the wavelength of the X-ray radiation, β is the full width at half maximum (FWHM) of

Table 1 Reagent usages for sample batch (mL)

Sample	0.005 mol/L	0.01214 mol/L	0.05 mol/L	0.05 mol/L
	ZnCl ₂	HAuCl ₄	FeSO ₃	NaOH
ZFA-11	1000	8.2	0	200
ZFA-12	1000	8.2	5	215
ZFA-13	1000	8.2	15	245
ZFA-14	1000	8.2	20	260
ZFA-15	1000	8.2	30	290

diffraction peak and θ is the scattering angle. The crystalline size is calculated in Table 2 in which we can find that Fe-decorated nanocrystals tend to be of little size.

Figure 2 shows SEM photographs of Au/Fe₂O₃-ZnO NPs. It could be found that samples have a good uniformity of particle size and morphology, and

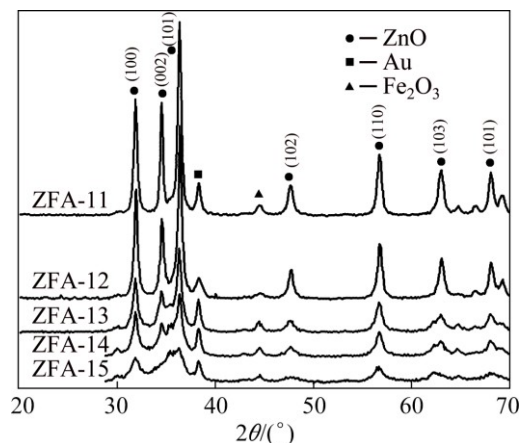


Fig. 1 XRD patterns of ZFA-11, ZFA-12, ZFA-13, ZFA-14 and ZFA-15 samples

Table 2 Crystalline size of samples (nm)

Sample	(100)	(002)	(101)	Average
ZFA-11	22.44	20.01	19.36	20.60
ZFA-12	20.22	28.56	20.93	23.24
ZFA-13	13.61	9.81	14.20	11.54
ZFA-14	12.43	6.39	8.86	9.23
ZFA-15	7.41	3.21	15.31	8.64

the particle size decreases from about 20 nm to 8 nm with increasing Fe content, which is well identical with the calculation results using XRD data (Table 2). This tiny particle size and the morphology uniformity might be achieved by two factors. First, microwave irradiation provided a very even and effective heat treatment to each sample, and the limited heating time reduced the crystal growth process. Furthermore, Fe₂O₃ NPs that formed during precipitation process and located in the surface of ZnO NPs inhibited ZnO particles aggregating to large size.

3.2 Gas-sensing performance

More studies have reported that the response of

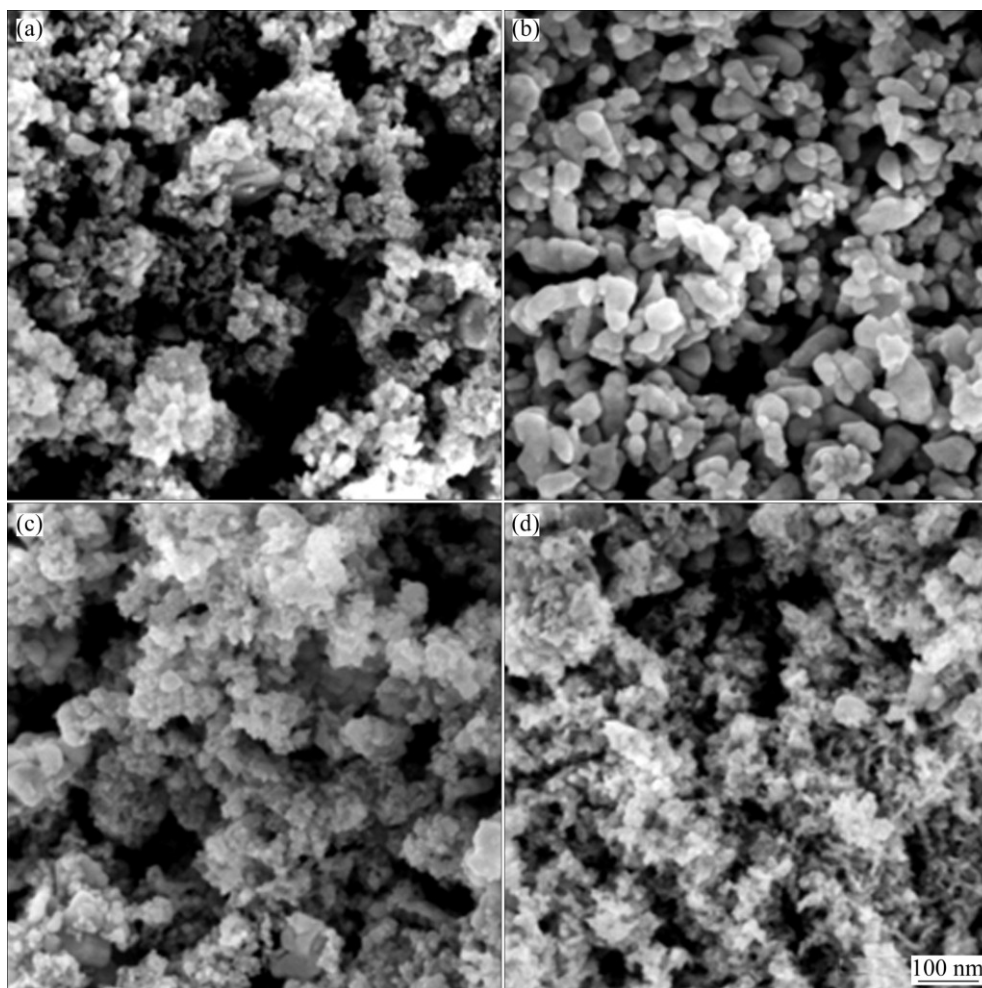


Fig. 2 SEM photographs of ZFA-11 (a), ZFA-12 (b), ZFA-13 (c) and ZFA-14 (d) samples

metal-oxide-semiconductor gas sensors mainly depends on the operating temperature. Therefore, it is necessary to investigate the optimum operating temperature of all sensors based on Au/Fe₂O₃-ZnO NPs. The responses of Au/Fe₂O₃-ZnO NPs to ethanol and acetone at different working temperatures from 210 to 390 °C are shown in Fig. 3. Figure 3(a) shows that gas responses of all sensors to ethanol increase to a maximum at about 300 °C, and then decrease with continuously increasing working temperature. It can be well concluded that the optimum working temperature of all sensors based on Au/Fe₂O₃-ZnO NPs towards ethanol is 300 °C. Meanwhile, Fig. 3(b) shows that responses of all Au/Fe₂O₃-ZnO based sensors towards acetone versus working temperature have same temperature dependence and a relatively low operating temperature (270 °C). In addition, it can be found that ZFA-11 and ZFA-13 sensors have the high response to ethanol (78) and acetone (90), respectively. This finding indicates that the Au/Fe₂O₃-ZnO sensors have the same gas-sensing process as semiconductor materials involve the adsorption and desorption of gases and the reaction of the adsorbed gases on the surface-active sites of the materials. Sufficient thermal energy is necessary across

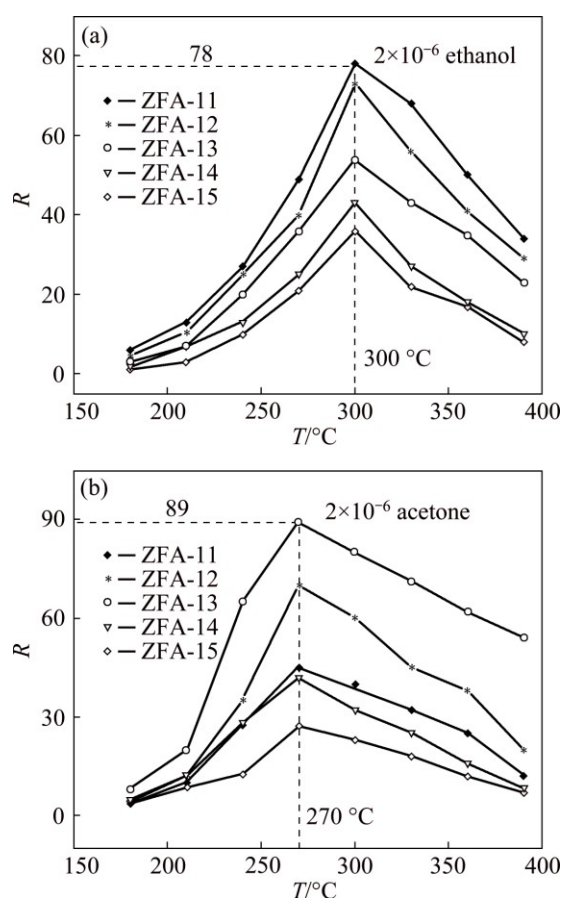


Fig. 3 Response (*R*) curves of ZFA-11, ZFA-12, ZFA-13, ZFA-14 and ZFA-15 samples versus working temperature (*T*) to ethanol gas (a) and to acetone gas (b)

the activation energy barrier for chemisorption and reaction between adsorbed gases on the surface of materials. The amount of chemical-adsorbed gas molecules increases with increasing operating temperature, and a higher sensing response is obtained. The desorption process becomes dominant when the operating temperature increases further, which results in the decrease of the response. For examining the effect of Fe-decorating on the selectivity of the sensor, the curves of response versus Fe-decorating content are shown in Fig. 4. It is found that the response of Au/Fe₂O₃-ZnO to ethanol decreases with increasing Fe-decorating content; on the contrary, the response to acetone increases with increasing Fe-decorating content. This is an encouraging result that the selectivity of Au/Fe₂O₃-ZnO sensor to acetone and ethanol is highly enhanced, and the working temperature of the sensor to acetone is obviously decreased.

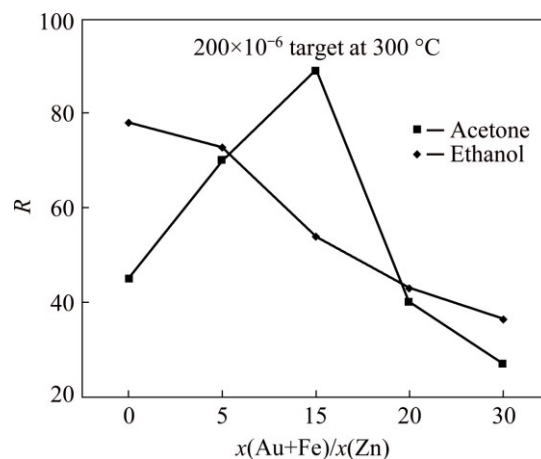


Fig. 4 Response of Au/Fe₂O₃-ZnO sensor to ethanol and acetone versus Fe-decorating content

Figure 5(a) shows the responses of Au/Fe₂O₃-ZnO NPs to ethanol in diverse contents ranging from 5 × 10⁻⁶ to 5 × 10⁻⁴. ZFA-11 based sensor shows preferable gas sensing performances to ethanol. And the gas responses decrease with increasing Fe-decorating content. It is indicated that the responses obviously increase with raising the ethanol content. The responses of ZFA-11 based sensor to 5 × 10⁻⁶, 10 × 10⁻⁶, 20 × 10⁻⁶, 50 × 10⁻⁶, 100 × 10⁻⁶, 200 × 10⁻⁶ and 500 × 10⁻⁶ ethanol are 9.5, 13.5, 19, 34, 52, 78 and 132, respectively, as shown in Fig. 6(a). It is proven that the decorating of Fe restrains the adsorption and desorption of target gas. Figure 5(b) illustrates the responses of Au/Fe₂O₃-ZnO NPs to acetone in diverse contents ranging from 5 × 10⁻⁶ to 500 × 10⁻⁶. ZFA-13 based sensor shows the highest gas response to acetone, and has good selectivity to ethanol and acetone. The gas sensitivities increase quickly at first, and then shift down with the continuously increasing Fe content. The responses of ZFA-13 based sensor to

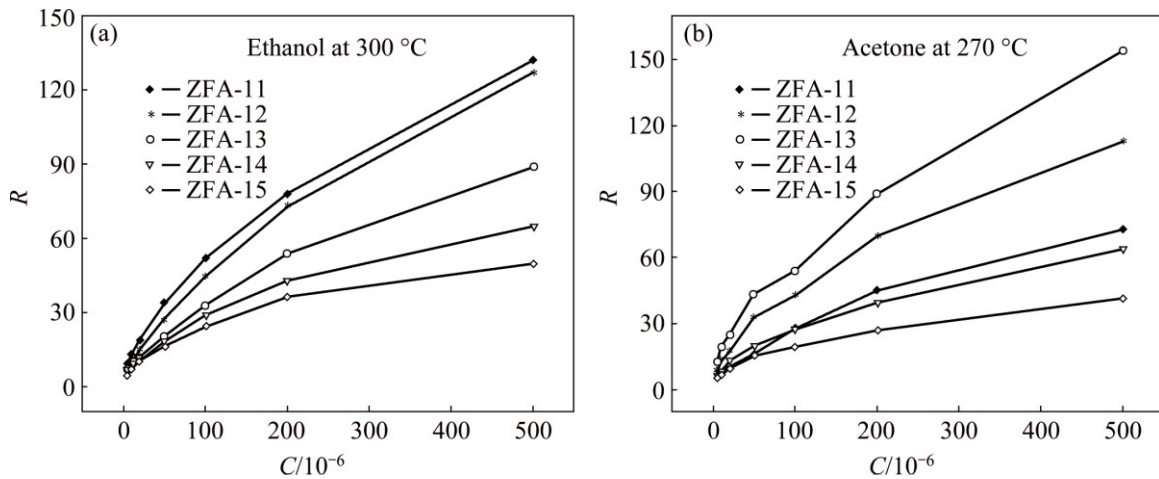


Fig. 5 Response (R) curves of ZFA-11, ZFA-12, ZFA-13, ZFA-14 and ZFA-15 samples versus gas content (C) to ethanol gas (a) and to acetone gas (b)

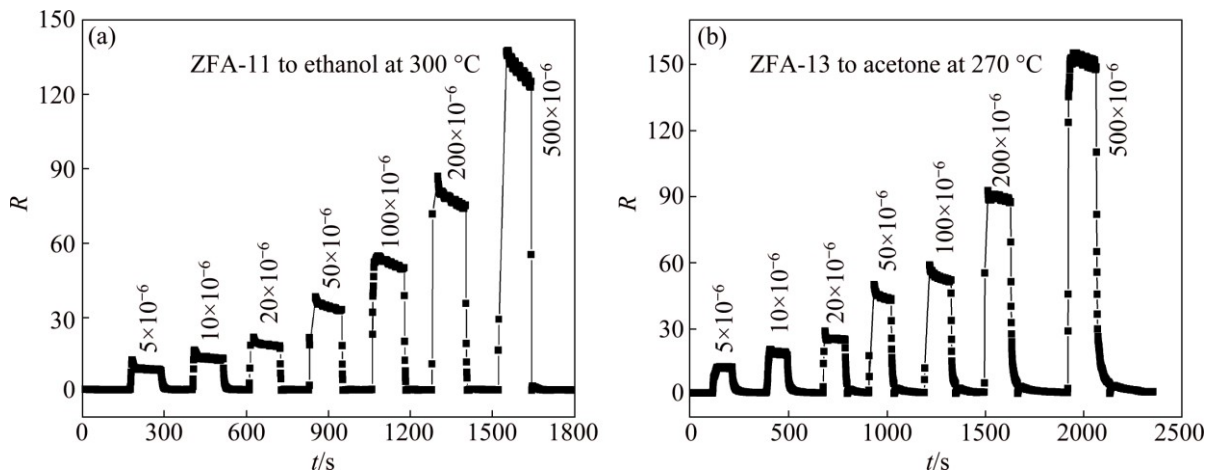


Fig. 6 Response (R) curves of ZFA-11 based sensor to ethanol gas at 300 °C (a) and ZFA-13 based sensor to acetone gas at 270 °C (b)

acetone contents ranging from 5×10^{-6} to 500×10^{-6} are 12.5, 19.5, 25, 43.5, 54, 89 and 154, as shown in Fig. 6(b). The decorating of Au and Fe promotes the adsorption on the surface of sensors, and changes the surface conductivity of ZnO. This sensor can be well used in low acetone content.

Figure 7 shows responses of ZFA-11, ZFA-12, ZFA-13, ZFA-14 and ZFA-15 toward 200×10^{-6} ethanol (C_2H_6O), acetone (C_3H_6O), methanol (CH_4O), benzene (C_6H_6), methylbenzene (C_7H_8), hydrogen (H_2), ammonium (NH_3), carbon monoxide (CO), and methane (CH_4) at working temperature of 300 °C. It can be seen that the highest response target gas of ZFA-11 based sensor is ethanol among all these testing gases, and the response decreases with continuously increasing Fe-decorating content. The response of ZFA-13 based sensor to acetone is the highest among all the sensors. However, the response increases when $x(Au+Fe)/x(Zn)$ ratio changes from 5% to 15%, and then it decreases with

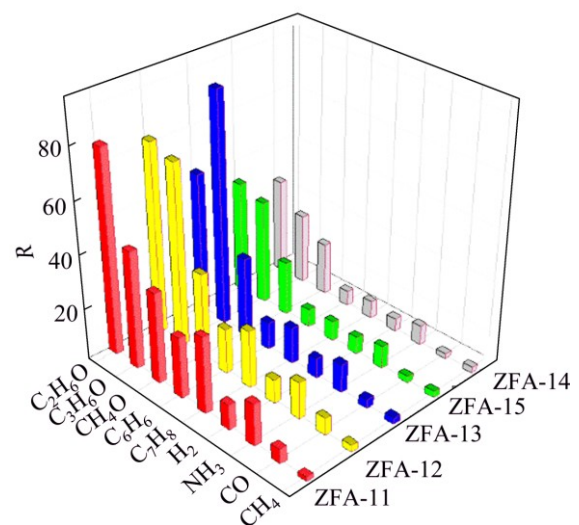


Fig. 7 Diagrams of responses of ZFA-11, ZFA-12, ZFA-13, ZFA-14 and ZFA-15 toward different target gases with content of 2×10^{-4} at 300 °C

increasing Fe content. The response of ZFA-13 based sensor to acetone is 1.6, 2.9, 6.3 times that to ethanol, methanol and methylbenzene, respectively, and it is more than 8.5 times that of other gases. This indicates that decorating with Au and Fe can effectively improve the gas sensitivity, and ZFA-13 with Au to Zn molar ratio of 2% and (Au+Fe) to Zn molar ratio of 15% can be well used to detect acetone, and also used in the application of ethanol, methanol and methylbenzene sensors.

Figure 8 shows the resistance changes of ZFA-11 and ZFA-13 alternately exposed to air and 2×10^{-4} target gases. We can see that both samples exhibit fast response after target gases are injected, and reach the equilibrium value over a relatively short time. It is indicated that the response and recovery time of ZFA-11 based sensor to ethanol at 300 °C are 1 and 9 s, and those of ZFA-13 based sensor to acetone at 270 °C are 1 and 32 s. These sensors have a quick response and a relatively quick recovery speed. The reliability test of the Au/Fe₂O₃-ZnO based sensors was carried out at their optimum operating temperature against 2×10^{-4} target gases. Five testing cycles of ZFA-11 and ZFA-13 sensors were recorded. By decorating Au and Fe in ZnO, primary energy levels are changed, and the degree of releasing trapped electrons is greater than that without decorating, which results in larger decrease of electrical resistance. Therefore, the gas sensing properties of ZnO nanoparticles are improved.

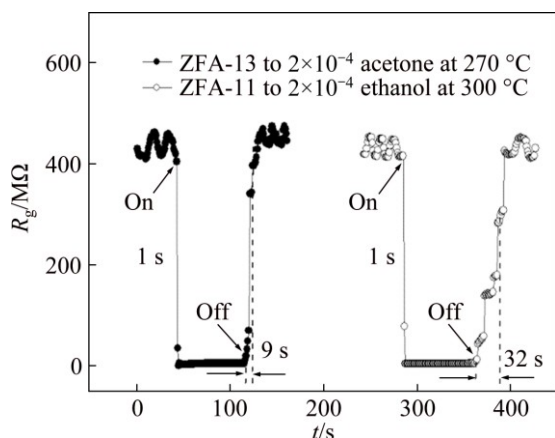


Fig. 8 Responses and recovery time of ZFA-11 and ZFA-13 based sensors against 2×10^{-4} ethanol and acetone at their optimum operating temperature

It can be seen in Fig. 9 that the responses have no reduction even after five cycle tests. So, the Au/Fe₂O₃-ZnO based sensor with good stability provides guidance for the large-scale practical application.

3.3 Gas-sensing mechanism of Au/Fe₂O₃-ZnO

It is well accepted that the gas-sensing mechanism of ZnO-based sensors belongs to surface-controlled type. The gas performance of ZnO is influenced by many

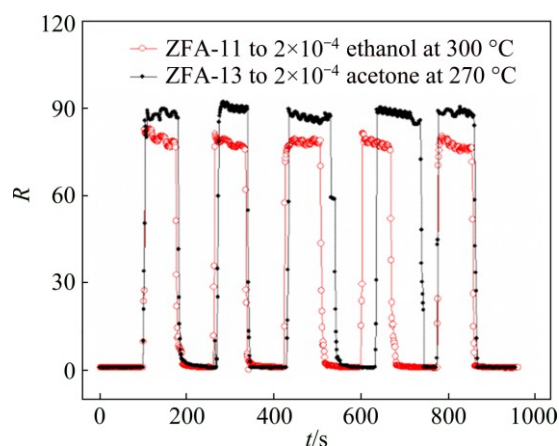
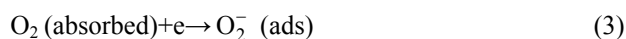


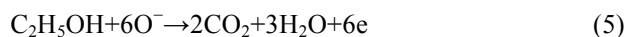
Fig. 9 Reliability tests of gas-sensing performance of ZFA-11 and ZFA-13 based sensors toward 2×10^{-4} ethanol and acetone at their optimum operating temperature

different factors and depends on the change of electrical resistance of the sensor materials in the presence of target gases. The oxidation of the surface releases electrons and increases the charge in the conduction band of the n-type oxide, and hence the conductivity gets increased. The extent of adsorbed oxygen ions and existence of their different chemical forms (O^- or O^{2-}) on the sensor surface are controlled by the sensor operating temperature. The gas sensing process can be understood by two distinct reaction stages [27]:

1) Firstly, sensor materials absorb oxygen molecules to produce oxygen ions, which causes the decrease of charge carriers (free electron in ZnO bulk) to reduce the conductivity:



2) Then target gases absorbed on the surface of the gas-sensing materials react with the absorbed oxygen molecules to release the captured electrons to return to ZnO particles. The oxidation reactions of C₂H₅OH and C₃H₆O can be represented as follows:



Introducing Au and Fe₂O₃ nanoparticles into ZnO NPs could lead to (1) the decrease of activation energy between adsorbed oxygen and the semiconductor surface, which reduces the operating temperature; (2) the increase of the amount of the adsorbed oxygen species on ZnO, therefore strengthening the interactions between the target gases and the adsorbed ionized oxygen, and then increasing the electric conductivity. The interaction between ZnO with Au/Fe NPs brings out the role of Au/Fe as modulator of the surface electronic structure, which leads to a higher value of surface electrical

resistance in air. When this Au/Fe₂O₃-ZnO sensor is exposed to ethanol, acetone or other reducing target gas, ethanol or acetone gets converted to CO₂ and H₂O by utilizing the surface adsorbed oxygen species and releasing electrons, leading to an increase in electric conductivity. The Au/Fe₂O₃-ZnO is composed of numerous ZnO NPs and a looser nanostructure in comparison with the conventional tightly-contacted particles, which contributes to the diffusion and transport of gas in the sensing layer and makes both the outer and inner surfaces of ZnO NPs accessible to target gas molecules. In addition, the decorating of Au/Fe is most probably responsible for the change of resistance in the target gases: the adsorbed oxygen can diffuse faster to surface vacancies and capture electrons from the conduction band of ZnO NPs to produce oxygen ions (O⁻ or O²⁻). This increases the quantity of adsorbed oxygen and the molecule-ion conversion rate, which results in the greater and faster degree of electron depletion from the Au/Fe₂O₃-ZnO interface than that in pure ZnO. Meanwhile, the valence state of Fe ion can change between Fe³⁺ and Fe²⁺ while the sensor is switched from air to target gas, which causes more electrons to transfer to devote high gas response. Because the degree of Fe valence state change is related to target-gas type, the selectivity of the gas sensing materials can be increased by adding Fe₂O₃ in suitable content.

4 Conclusions

1) Ternary Au/Fe₂O₃-ZnO nanoparticles are successfully synthesized by a combining process of simple co-precipitation, microwave irradiation and heat treatment.

2) The as-prepared products consist of hexagonal wurtzite ZnO, face-centered cubic gold metal nanoparticles and orthorhombic crystalline Fe₂O₃ in several nanometer scales.

3) The sensors based on Au/Fe₂O₃-ZnO NPs have an extremely high response and an excellent selectivity to ethanol and acetone. The selectivity could be adjusted by Fe₂O₃ content added in the ternary materials.

References

- [1] GONZALEZ-JIMENEZ J, MONROY J G, BLANCO J L. The multi-chamber electronic nose—An improved olfaction sensor for mobile robotics [J]. *Sensors*, 2011, 11: 6145–6164.
- [2] KUANG S, BURRIS J F, NEWCHURCH M J, JOHNSON S, LONG S. Differential absorption lidar to measure subhourly variation of tropospheric ozone profiles [J]. *IEEE Transactions on Geoscience and Remote Sensing*, 2011, 49: 557–571.
- [3] GUO J, ZHANG J, GONG H B, JU D X, CAO B Q. Au nanoparticle-functionalized 3D SnO₂ microstructures for high performance gas sensor [J]. *Sensors and Actuators B—Chemical*, 2016, 226: 266–272.
- [4] SONG H J, SUN Y L, JIA X H. Hydrothermal synthesis, growth mechanism and gas sensing properties of Zn-doped alpha-Fe₂O₃ microcubes [J]. *Ceramics International*, 2015, 41: 13224–13231.
- [5] BOROUN Z, GHORBANI M, MOOSAVI A, MOHAMMADPOUR R. New insight into H₂S sensing mechanism of continuous SnO₂-CuO bilayer thin film: A theoretical macroscopic approach [J]. *Journal of Physical Chemistry C*, 2016, 120: 7678–7684.
- [6] WANG Y R, LIU B, XIAO S H, WANG X H, SUN L M, LI H, XIE W Y, LI Q H, ZHANG Q, WANG T H. Low-temperature H₂S detection with hierarchical Cr-doped WO₃ microspheres [J]. *ACS Applied Materials & Interfaces*, 2016, 8: 9674–9683.
- [7] WANG Y T, WHANG W T, CHEN C H. Hollow V₂O₅ nanoassemblies for high-performance room-temperature hydrogen sensors [J]. *ACS Applied Materials & Interfaces*, 2015, 7: 8480–8487.
- [8] LI Y, LIU J C, LIAN X X, LU T, ZHAO F X. Morphology, photoluminescence and gas sensing of Ce-doped ZnO microspheres [J]. *Transactions of Nonferrous Metals Society of China*, 2015, 25: 3657–3663.
- [9] JIANG X H, MA S Y, LI W Q, WANG T T, JIN W X, LUO J, CHENG L, MAO Y Z, ZHANG M. Synthesis of hierarchical ZnO nanostructure assembled by nanorods and their performance for gas sensing [J]. *Materials Letters*, 2015, 142: 299–303.
- [10] HU J, GAO F Q, ZHAO Z T, SANG S B, LI P W, ZHANG W D, ZHOU X T, CHEN Y. Synthesis and characterization of cobalt-doped ZnO microstructures for methane gas sensing [J]. *Applied Surface Science*, 2016, 363: 181–188.
- [11] ZOU A L, QIU Y, YU J J, YIN B, CAO G Y, ZHANG H Q, HU L Z. Ethanol sensing with Au-modified ZnO microwires [J]. *Sensors and Actuators B—Chemical*, 2016, 227: 65–72.
- [12] TEFAMICHAEL T, CETIN C, PILOTO C, ARITA M, BELL J. The effect of pressure and W-doping on the properties of ZnO thin films for NO₂ gas sensing [J]. *Applied Surface Science*, 2015, 357: 728–734.
- [13] JIN W X, MA S Y, TIE Z Z, XU X L, JIANG X H, LI W Q, WANG T T, LU Y, YAN S H. Synthesis of monodisperse ZnO hollow six-sided pyramids and their high gas-sensing properties [J]. *Materials Letters*, 2015, 159: 102–105.
- [14] WANG Y Y, DUAN G T, ZHU Y D, ZHANG H W, XU Z K, DAI Z F, CAI W P. Room temperature H₂S gas sensing properties of In₂O₃ micro/nanostructured porous thin film and hydrolyzation-induced enhanced sensing mechanism [J]. *Sensors and Actuators B—Chemical*, 2016, 228: 74–84.
- [15] CHEN M, WANG Z H, HAN D M, GU F B, GUO G S. Porous ZnO polygonal nanoflakes: Synthesis, use in high-sensitivity NO₂ gas sensor, and proposed mechanism of gas sensing [J]. *Journal of Physical Chemistry C*, 2011, 115: 12763–12773.
- [16] SINHA M, MAHAPATRA R, MONDAL B, MARUYAMA T, GHOSH R. Ultrafast and reversible gas-sensing properties of ZnO nanowire arrays grown by hydrothermal technique [J]. *Journal of Physical Chemistry C*, 2016, 120: 3019–3025.
- [17] SUN G, ZHANG S S, LI Y W, QI F X, CHEN H L, ZHANG Z Y. Core-shell ZnO/SnO₂ nanorods: Two-step synthesis and enhanced ethanol sensing performance [J]. *Current Nanoscience*, 2015, 11: 405–412.
- [18] LI Y, LV T, ZHAO F X, LIAN X X, ZOU Y L, WANG Q. Polarity-enhanced gas-sensing performance of Au-loaded ZnO nanospindles synthesized via precipitation and microwave irradiation [J]. *Electronic Materials Letters*, 2016, 12: 411–418.
- [19] NA H G, KWON Y J, CHO H Y, KANG S Y, KIM H W. Improvement of gas sensing characteristics by adding Pt nanoparticles on ZnO-branched SnO₂ nanowires [J]. *Journal of Nanoscience and Nanotechnology*, 2015, 15: 8571–8576.
- [20] WANG Z H, TIAN Z W, HAN D M, GU F B. Highly sensitive and

- selective ethanol sensor fabricated with In-doped 3DOM ZnO [J]. ACS Applied Materials & Interfaces, 2016, 8: 5466–5474.
- [21] SUO C, GAO C J, WU X Y, ZUO Y, WANG X C, JIA J F. Ag-decorated ZnO nanorods prepared by photochemical deposition and their high selectivity to ethanol using conducting oxide electrodes [J]. RSC Advances, 2015, 5: 92107–92113.
- [22] YAN S H, MA S Y, LI W Q, XU X L, CHENG L, SONG H S, LIANG X Y. Synthesis of SnO₂-ZnO heterostructured nanofibers for enhanced ethanol gas-sensing performance [J]. Sensors and Actuators B-Chemical, 2015, 221: 88–95.
- [23] LI X W, ZHOU X, GUO H, WANG C, LIU J Y, SUN P, LIU F M, LU G Y. Design of Au@ZnO yolk-shell nanospheres with enhanced gas sensing properties [J]. ACS Applied Materials & Interfaces, 2014, 6: 18661–18667.
- [24] HAN L N, WANG D J, LU Y C, JIANG T F, LIU B K, LIN Y H. Visible-light-assisted HCHO gas sensing based on Fe-doped flowerlike ZnO at room temperature [J]. Journal of Physical Chemistry C, 2011, 115: 22939–22944.
- [25] MIRZAEI A, PARK S, KHEEL H, SUN G J, LEE S, LEE C. ZnO-capped nanorod gas sensors [J]. Ceramics International, 2016, 42: 6187–6197.
- [26] LIANG Y C, LIAO W K, DENG X S. Synthesis and substantially enhanced gas sensing sensitivity of homogeneously nanoscale Pd- and Au-particle decorated ZnO nanostructures [J]. Journal of Alloys and Compounds, 2014, 599: 87–92.
- [27] GARDON M, GUILMANY J M. A review on fabrication, sensing mechanisms and performance of metal oxide gas sensors [J]. Journal of Materials Science–Materials in Electronics, 2013, 24: 1410–1421.

三元 Au/Fe₂O₃-ZnO 基高选择性丙酮气敏材料的共沉淀和微波辐照法合成

李 甦, 陈丽丽, 赵方贤

中国民航大学 理学院, 天津 300300

摘 要: 采用共沉淀和微波辐照法合成三元 Au/Fe₂O₃-ZnO 基气敏材料。采用 X 射线衍射仪和扫描电子显微镜对材料进行表征, 并对其气敏性能进行测试。结果表明, 材料由六方纤锌矿 ZnO、面心立方纳米金和斜方相 Fe₂O₃ 晶粒组成。Au/Fe₂O₃-ZnO 基传感器对乙醇和丙酮具有很高的选择性, 在较低工作温度(270 °C)下, 对丙酮气体的灵敏度高(154), 且响应速度极快(1 s)。材料对气体的选择性与加入该材料的 Fe₂O₃ 量有关。该材料在丙酮气体检测与安全管理方面具有非常好的应用前景。

关键词: 氧化锌; 氧化铁; 金; 丙酮传感器; 乙醇传感器

(Edited by Bing YANG)